

# The Human Heart and Rat Brain IIA Na<sup>+</sup> Channels Interact with Different Molecular Regions of the $\beta_1$ Subunit

THOMAS ZIMMER and KLAUS BENNDORF

Friedrich Schiller University Jena, Institute of Physiology II, Teichgraben 8, 07740 Jena, Germany

**ABSTRACT** The  $\alpha$  subunit of voltage-gated Na<sup>+</sup> channels of brain, skeletal muscle, and cardiomyocytes is functionally modulated by the accessory  $\beta_1$ , but not the  $\beta_2$  subunit. In the present study, we used  $\beta_1/\beta_2$  chimeras to identify molecular regions within the  $\beta_1$  subunit that are responsible for both the increase of the current density and the acceleration of recovery from inactivation of the human heart Na<sup>+</sup> channel (hH1). The channels were expressed in *Xenopus* oocytes. As a control, we coexpressed the  $\beta_1/\beta_2$  chimeras with rat brain IIA channels. In agreement with previous studies, the  $\beta_1$  extracellular domain sufficed to modulate IIA channel function. In contrast to this, the extracellular domain of the  $\beta_1$  subunit alone was ineffective to modulate hH1. Instead, the putative membrane anchor plus either the intracellular or the extracellular domain of the  $\beta_1$  subunit was required. An exchange of the  $\beta_1$  membrane anchor by the corresponding  $\beta_2$  subunit region almost completely abolished the effects of the  $\beta_1$  subunit on hH1, suggesting that the  $\beta_1$  membrane anchor plays a crucial role for the modulation of the cardiac Na<sup>+</sup> channel isoform. It is concluded that the  $\beta_1$  subunit modulates the cardiac and the neuronal channel isoforms by different molecular interactions: hH1 channels via the membrane anchor plus additional intracellular or extracellular regions, and IIA channels via the extracellular region only.

**KEY WORDS:**  $\beta_2$  subunit • cardiac electrophysiology • Na<sub>v</sub>1.2 • Na<sub>v</sub>1.5 • subunit interaction

## INTRODUCTION

Voltage-gated sodium (Na<sup>+</sup>) channels are responsible for the initiation and propagation of action potentials in electrically excitable cells (Catterall, 1992). These channels are heteromultimeric proteins of the plasma membrane consisting of a pore-forming  $\alpha$  subunit and accessory  $\beta$  subunits. Screening for cDNAs encoding Na<sup>+</sup> channel subunits revealed the existence of 10  $\alpha$  and 3  $\beta$  subunit isoforms in mammalian cells (Goldin, 2001).

As demonstrated by heterologous expression experiments, the  $\alpha$  subunit determines the main electrophysiological and pharmacological properties of a given Na<sup>+</sup> channel complex (Catterall, 1992), while two of the three  $\beta$  subunits ( $\beta_1$  and  $\beta_3$ ) modulate the function of the  $\alpha$  subunits (Patton et al., 1994; Morgan et al., 2000). When expressed in *Xenopus* oocytes, the  $\beta_1$  subunit increases the current amplitude and accelerates the recovery from inactivation in currents generated by cardiac (Nuss et al., 1995; Qu et al., 1995), skeletal muscle (Wallner et al., 1993; Yang et al., 1993; Makita et al., 1994) and neuronal Na<sup>+</sup> channels (Isom et al., 1992; Smith and Goldin, 1998; Vijayaragavan et al., 2001). In addition to this, neuronal and skeletal muscle Na<sup>+</sup> channels require the  $\beta_1$  subunit for fast inactivation (Isom et al., 1992; Wallner et al., 1993; Yang et al., 1993;

Makita et al., 1994; Patton et al., 1994; Nuss et al., 1995; Smith and Goldin, 1998; Vijayaragavan et al., 2001).

The molecular mechanisms leading to the increased current densities and to the accelerated recovery from inactivation have not been elucidated. Recent data indicate that the human heart Na<sup>+</sup> channel (hH1; Gellens et al., 1992) assembles with the  $\beta_1$  subunit already within the endoplasmic reticulum (Zimmer et al., 2002). This may result in an improved trafficking of the channel complex to the plasma membrane, similarly as reported for ATP-sensitive K<sup>+</sup> channels (Zerangue et al., 1999). Single-channel experiments with hH1 indicated that the larger current amplitude upon  $\beta_1$  coexpression is not due to a change of the channel open probability (Nuss et al., 1995). Together, these data suggest that increased current amplitudes are due to an increase of the number of functional channels in the plasma membrane. In this context, it is interesting to note that Na<sup>+</sup> channel  $\beta$  subunits are highly homologous to cell adhesion molecules (CAM) of the Ig superfamily (Isom et al., 1995; Isom, 2001). Their extracellular domains bind to extracellular matrix molecules (Srinivasan et al., 1998; Xiao et al., 1999), strongly suggesting a function of Na<sup>+</sup> channel  $\beta$  subunits in promoting cell-cell contacts and in modulating localization and cell-surface density of  $\alpha$  subunits.

Molecular regions of the  $\beta_1$  subunit that are responsible for the modulation of the electrophysiological properties of IIA and human skeletal muscle (hSKM1) Na<sup>+</sup> channels are located within the extracellular do-

Address correspondence to Thomas Zimmer, Friedrich Schiller University, Jena Institute of Physiology II, Teichgraben 8, 07740 Jena, Germany. Fax: (49) 3641-933202; E-mail: tzim@mti-n.uni-jena.de

main (Chen and Cannon, 1995; McCormick et al., 1998, 1999). In these studies it was shown that neither the putative  $\beta_1$  membrane anchor nor the  $\beta_1$  intracellular domain is required for the  $\beta_1$ -like modulation of sodium channel gating. This result was further substantiated by the finding that the corresponding  $\beta_1$  subunit response element in IIA and hSKM1 channels is localized within an extracellular loop (domain IV, loop S5/S6; Makita et al., 1996; Qu et al., 1999).

In the present study we used chimeras and deletion variants of  $\beta_1$  and  $\beta_2$  subunits to identify  $\beta_1$  mo-

lecular regions involved in the modulation of hH1. We show that—in contrast to the result with IIA channels—the  $\beta_1$  extracellular domain is neither sufficient nor necessary for the  $\beta_1$  effect on the recovery kinetics and current density of hH1 channels expressed in *Xenopus* oocytes. Instead, the putative membrane anchor plus either the extracellular or the intracellular domain of the  $\beta_1$  subunit are required to modulate hH1. We conclude that hH1 and IIA channels interact specifically with different molecular regions of the  $\beta_1$  subunit.

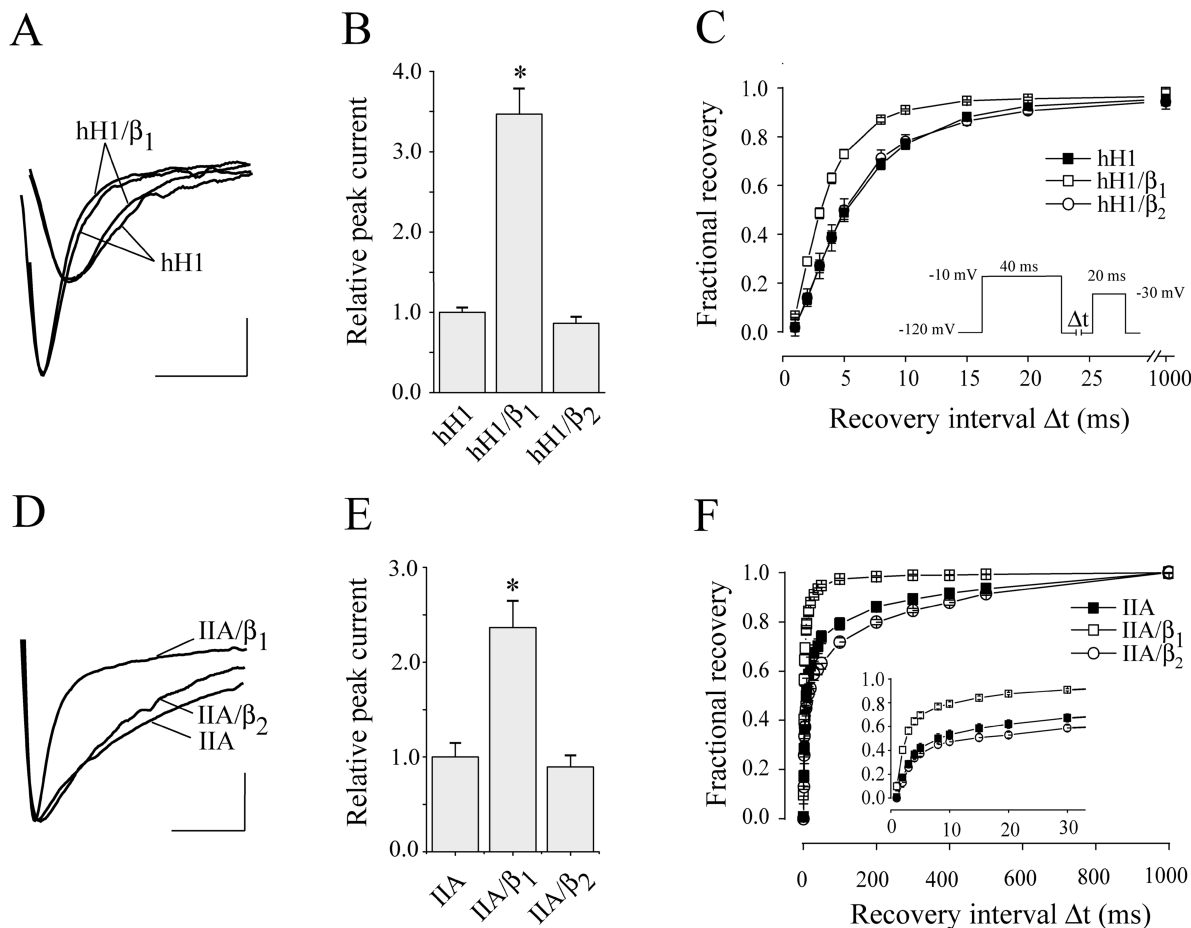


FIGURE 1. Modulation of hH1 and IIA  $\text{Na}^+$  channels by the  $\beta_1$  subunit. (A) Representative current traces for hH1 and hH1/ $\beta_1$  channels at the test potentials  $-10$  and  $-30$  mV. The  $\tau_h$  values of hH1 versus hH1/ $\beta_1$  channels were statistically indistinguishable ( $-30$  mV:  $\tau_h = 2.21 \pm 0.18$  for hH1,  $\tau_h = 2.01 \pm 0.43$  for hH1/ $\beta_1$  [ $P = 0.64$ ];  $-10$  mV:  $\tau_h = 1.25 \pm 0.07$  for hH1,  $\tau_h = 1.12 \pm 0.08$  for hH1/ $\beta_1$  [ $P = 0.23$ ]). Number of experiments:  $n = 11$  for hH1,  $n = 6$  for hH1/ $\beta_1$ . Calibration bars = 4 ms, at  $-30$  mV:  $0.25 \mu\text{A}$  for hH1,  $0.62 \mu\text{A}$  for hH1/ $\beta_1$ ; at  $-10$  mV:  $0.45 \mu\text{A}$  for hH1,  $1.06 \mu\text{A}$  for hH1/ $\beta_1$ . (B) Effect of the  $\beta_1$  subunit on the hH1 peak current amplitude in *Xenopus* oocytes ( $*P < 0.001$ ). Currents were measured 3 d after injection at the test potential of  $-25$  mV. Measurements were performed in seven different batches of oocytes. Data from a single batch of oocytes were normalized with respect to the mean current of hH1-injected oocytes ( $n = 63$  for hH1,  $n = 50$  for hH1/ $\beta_1$ , and  $n = 52$  for hH1/ $\beta_2$ ). (C) Time course of recovery from inactivation of hH1 channels. The respective voltage protocol is shown in the inset ( $n = 32$  for hH1,  $n = 38$  for hH1/ $\beta_1$ , and  $n = 21$  for hH1/ $\beta_2$ ). (D) Effect of the  $\beta_1$  subunit on the inactivation time course of rat brain IIA  $\text{Na}^+$  currents. The  $\text{Na}^+$  currents were elicited by a test pulse to  $-10$  mV, and normalized with respect to the peak current. Calibration bars = 5 ms,  $0.9 \mu\text{A}$  for IIA,  $0.8 \mu\text{A}$  for IIA/ $\beta_1$ , and  $0.7 \mu\text{A}$  for IIA/ $\beta_2$ . Statistically, the inactivation time constant  $\tau_h$  was not different for IIA and IIA/ $\beta_2$  channels at the applied test pulses (unpublished data). (E) Effect of the  $\beta_1$  subunit on the IIA peak current amplitude ( $*P < 0.001$ ). Currents were measured 3 d after injection at the test potential of  $-10$  mV ( $n = 13$  for IIA,  $n = 13$  for IIA/ $\beta_1$  and  $n = 13$  for IIA/ $\beta_2$ ). (F) Time course of recovery from inactivation of IIA channels. Currents were elicited by the same voltage protocol as indicated in C, except that a test pulse to  $-10$  mV was used ( $n = 7$  for IIA,  $n = 7$  for IIA/ $\beta_1$  and  $n = 6$  for IIA/ $\beta_2$ ). Bars indicate SEM.

*cDNAs of Na<sup>+</sup> Channel Subunits*

Plasmids pSP64T-hH1, pNa200, and pSPNaβ coding for hH1 (EMBL/GenBank/DDBJ accession no. M77235; Gellens et al., 1992), for the rat brain IIA Na<sup>+</sup> channel (EMBL/GenBank/DDBJ accession no. X61149; Auld et al., 1988) and for the rat β<sub>1</sub> subunit (EMBL/GenBank/DDBJ accession no. M91808; Isom et al., 1992) were provided by A.L. George (Vanderbilt University), A.L. Goldin (University of California) and W. Stühmer (Max Planck Institute, Göttingen), respectively. The β<sub>2</sub> subunit (EMBL/GenBank/DDBJ accession no. U37026, Isom et al., 1995) was isolated by RT-PCR from the human brain astrocytoma cell line 1321N1, as already described (Zimmer et al., 2002).

*Recombinant DNA Procedures*

To obtain a comparable translation efficiency of the different β subunit variants in *Xenopus* oocytes, we subcloned each of the β subunit constructs into the same in vitro transcription vector (pGEMHEnew; Liman et al., 1992). This vector contains the T7 promoter, a 5'-untranslated region (UTR)\* of the *Xenopus* β-globin gene, a multicloning site (mcs) used to insert the β subunit variants, and a 3'-UTR of the *Xenopus* β-globin gene. Since this 3'-UTR is not present in the hH1-containing vector pSP64T-hH1, we linearized all β subunit plasmids for in vitro transcription using a restriction site within the mcs downstream to the β subunit sequence so that also the resulting cRNAs did not contain the β-globin 3'-UTR. Thus, the hH1 and each of the β subunit cRNAs were composed of the β-globin 5'-UTR and the hH1 or the respective β subunit sequences.

The β<sub>1</sub> cDNA was isolated from pSPNaβ and subcloned into pGEMHEnew using the HindIII-XbaI and EcoRI-XbaI sites, respectively, resulting in pGEM-β<sub>1</sub>. The HindIII and EcoRI sites were treated with Klenow enzyme to allow for blunt end ligation. The β<sub>2</sub> cDNA was inserted into the BamHI-HindIII site of pGEMHEnew, resulting in pGEM-β<sub>2</sub>, as described previously (Zimmer et al., 2002).

The β subunit chimeras constructed are shown in Fig. 2. To create the constructs β<sub>122</sub>, β<sub>211</sub>, β<sub>122a</sub>, β<sub>211a</sub>, and β<sub>221</sub>, the desired β<sub>1</sub> and β<sub>2</sub> subunit regions were first separately amplified by PCR and then linked by a recombinant PCR step (Higuchi, 1989) using the following internal primer pairs: 5'-CACCCACAATCTCTGACACCGATGGATGCCAT-3' and 5'-CGTGTGACAGATGTTGGGTGCTCCGTCGG-3' for the construction of β<sub>122</sub>, 5'-GGTGGCCGTGATCATGATGTACGTGCTCAT-3' and 5'-ACATCATGATCACGGCCACCGTGAAGTCCC-3' for the construction of β<sub>211</sub>, 5'-CCTGCAGATGGATCTTCTTGACGACGCTGG-3' and 5'-CAAGAAGATCCATCTGCAGGTCCTCATGGA-3' for the construction of β<sub>122a</sub>, 5'-TGGCAAGATCCACCTGGAGGTGGTGGCAA-3' and 5'-CCTCCAGGTGATCTTGCCATGGCCACCGGT-3' for the construction of β<sub>211a</sub>, and 5'-GGTGCTGATGGTGTACTGCTACAAGAAGAT-3' and 5'-AGCAGTACACCATCAGCACCAAGATGACCA-3' for the construction of β<sub>221</sub>. Recombinant fragments were subcloned into the BamHI-HindIII (β<sub>122</sub>, β<sub>122a</sub>) or Asp718-EcoRI sites (β<sub>211</sub>, β<sub>211a</sub>, β<sub>221</sub>) of pGEMHEnew, resulting in pGEM-β<sub>122</sub>, pGEM-β<sub>122a</sub>, and in pGEM-β<sub>211</sub>, pGEM-β<sub>211a</sub>, pGEM-β<sub>221</sub>, respectively. Chimeras β<sub>121</sub> and β<sub>212</sub> were created using the β<sub>122</sub> and β<sub>211</sub> constructs as initial templates for PCR and the following internal primer pairs: 5'-GGTGCTGATGGTGTACTGCTACAAGAAGAT-3' and 5'-AGCAGTACACCATCAGCACCAAGATGACCA-3' for the construction of β<sub>121</sub>, and 5'-ACTTGAC-

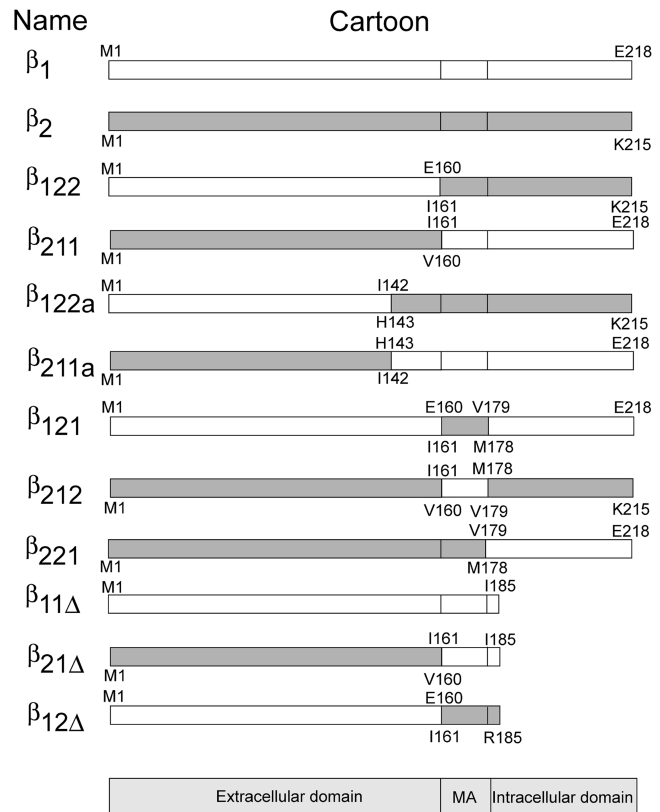


FIGURE 2. Structure of the chimeras between the Na<sup>+</sup> channel β<sub>1</sub> and β<sub>2</sub> subunits used in this study. The corresponding terminal amino acids of the β<sub>1</sub> (white boxes) and β<sub>2</sub> (gray boxes) subunit regions are indicated. The assumed topology of both subunits in the plasma membrane is shown below the cartoons of the chimeras.

CACCATCTCCGCCACGAGCCATA-3' and 5'-GGCGGAGATGTGGTCAAGTGTGTGAGGAG-3' for the construction of β<sub>212</sub>. Recombinant PCR fragments were subcloned into the Asp718-Bsp1407 (β<sub>121</sub>) and Asp718-Bpu1102 sites (β<sub>212</sub>) of pGEM-β<sub>1</sub> and pGEM-β<sub>2</sub>, resulting in pGEM-β<sub>121</sub> and pGEM-β<sub>212</sub>, respectively. The deletion variants β<sub>11Δ</sub> and β<sub>21Δ</sub> were constructed by PCR. For the introduction of a stop codon at the desired position (underlined in the primer sequence) and an XbaI site for the subsequent cloning step (indicated in italics in the primer sequence), we used oligonucleotide 5'-AAATCTAGACTAAATCTTCTGTAGCAGTACAC-3' as one of the flanking primers. The sequence of the T7 promoter in pGEM-β<sub>1</sub> and pGEM-β<sub>211</sub> served as the second primer site. The β<sub>11Δ</sub> and β<sub>21Δ</sub> PCR fragments were subcloned into the Asp718-XbaI site of pGEMHEnew, resulting in pGEM-β<sub>11Δ</sub> and pGEM-β<sub>21Δ</sub>, respectively. Construct β<sub>12Δ</sub> was also obtained by PCR. We used oligonucleotide 5'-AAAAAGCTTCAACCTGCTCTACCTCCTCACACATTGACCAC-3' (underlined: stop codon; italics: HindIII site) and the T7 promoter sequence to amplify the shortened chimera from plasmid pGEM-β<sub>122</sub>. The product was subcloned into the Asp718-HindIII site of pGEMHEnew, resulting in pGEM-β<sub>12Δ</sub>.

PfuTurbo DNA Polymerase (Stratagene) was used for all PCR reactions to minimize PCR-mediated nucleotide exchanges. The correctness of the DNA constructs was checked by the dideoxy DNA sequencing method. Preparation, digestion, and ligation of DNA were performed according to standard procedures (Sambrook et al., 1989).

\*Abbreviations used in this paper: ED, extracellular domain; ID, intracellular domain; MA, membrane anchor; UTR, untranslated region.

*Heterologous Expression in Xenopus Oocytes*

Capped cRNAs of hH1 and of IIA were prepared by SpeI and NotI digestion of plasmids pSP64T-hH1 and pNa200, respectively, followed by in vitro transcription reaction with SP6 (hH1) and T7 (IIA) RNA polymerase (Roche Diagnostics GmbH). Vectors pGEM- $\beta_2$ , pGEM- $\beta_{122}$ , pGEM- $\beta_{122\Delta}$ , pGEM- $\beta_{211}$ , pGEM- $\beta_{211\Delta}$ , pGEM- $\beta_{221}$ , pGEM- $\beta_{121}$ , pGEM- $\beta_{212}$ , and pGEM- $\beta_{21\Delta}$  were linearized by HindIII digestion, and vectors pGEM- $\beta_1$  and pGEM- $\beta_{11\Delta}$  were linearized by XbaI digestion. The in vitro transcription reaction was performed using T7 RNA polymerase.

Oocytes from *Xenopus laevis* were obtained as described previously (Zimmer et al., 2002). Glass micropipettes were used to inject a cRNA volume per oocyte of 40–60 nl. Concentrations of the different cRNA preparations were assessed by agarose gel electrophoresis using the 0.24–9.5 kb RNA ladder from GIBCO BRL. The hH1 and IIA cRNA preparations were injected at a final concentration of  $\sim 0.1 \mu\text{g}/\mu\text{l}$  and  $0.05 \mu\text{g}/\mu\text{l}$ , respectively. The different cRNAs encoding the  $\beta$  subunit variants were at a concentration of  $\sim 0.2 \mu\text{g}/\mu\text{l}$ . Thus, the final molar ratio of hH1 to  $\beta$  subunit variant

was  $\sim 1:20$  at the cRNA level. Injected oocytes were incubated for 3 d at  $18^\circ\text{C}$  in Barth medium. In control experiments, we tested the influence of the hH1/ $\beta_1$  cRNA ratio on current density and recovery from inactivation. Significant modulation of hH1 currents was already observed at a 1:1 ratio. The effects saturated at a ratio of 1:5 to 1:10, and were obtained also at higher  $\beta_1$  cRNA concentrations (1:40). However, only about one fifth of the  $\beta_1$  cRNA was required to modulate hH1 channels when incorporating the 3'-UTR of the  $\beta$ -globin sequence into the  $\beta_1$  cRNA (NotI digestion of pGEM- $\beta_1$ ). Current amplitudes did not increase when coinjecting undiluted  $\beta_1$  cRNA containing this  $\beta$ -globin sequence, although the recovery from inactivation of hH1 was clearly accelerated (unpublished data). A 3- to 10-fold dilution of this  $\beta_1$  cRNA containing both the 5'- and 3'-UTR of the *Xenopus*  $\beta$ -globin gene resulted in two- to fourfold higher peak current amplitudes accompanied by the described effect on the recovery kinetics. We think that this 3'-UTR enhances the translation efficiency of the  $\beta_1$  subunit. Thus, expression of hH1 whose cRNA does not contain this sequence is probably suppressed relative to the expression of  $\beta_1$ .

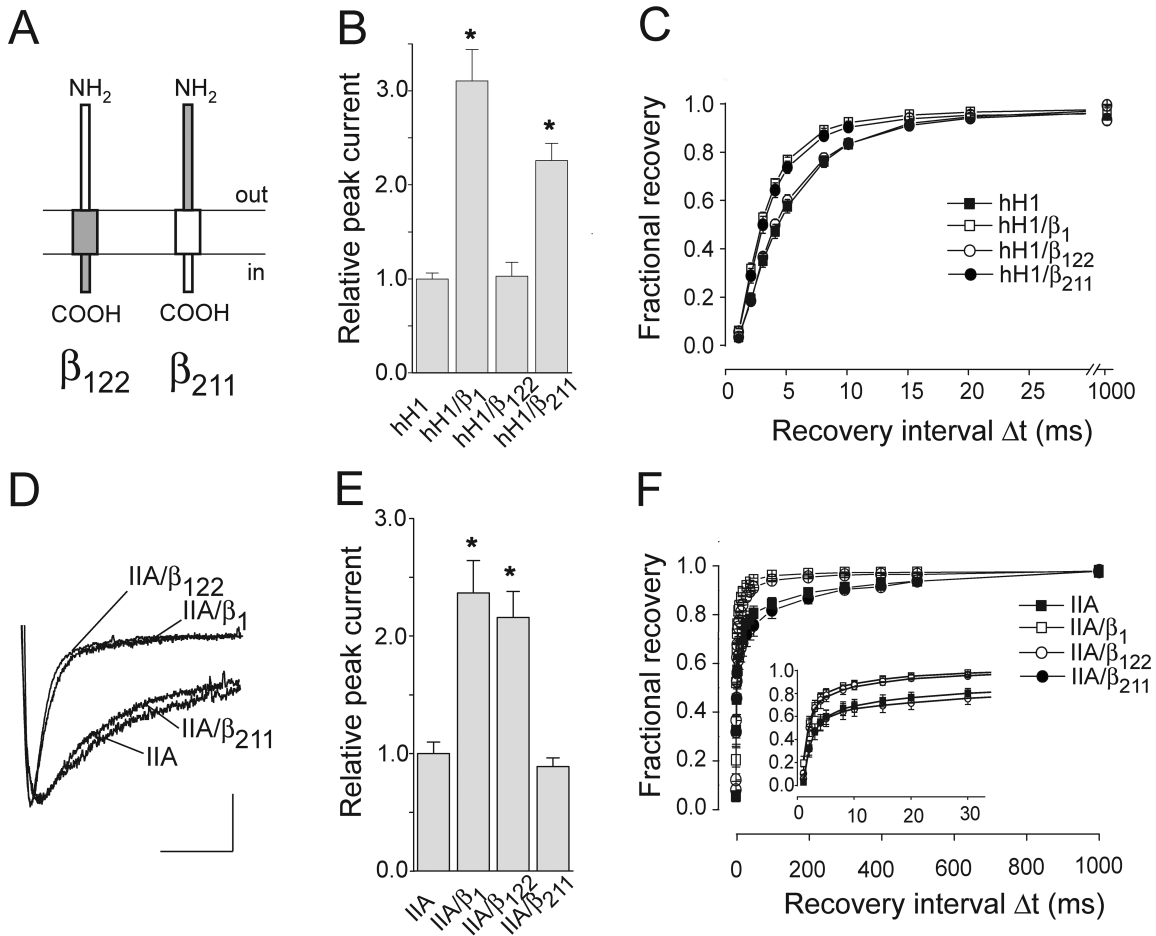


FIGURE 3. Modulatory effect of chimeras  $\beta_{122}$  and  $\beta_{211}$  on hH1 and IIA channels. (A) Schematic representation of the domain structures of both chimeras. (B) Relative current amplitudes (test pulse to  $-25$  mV;  $*P < 0.001$ ;  $n = 55$  for hH1,  $n = 37$  for hH1/ $\beta_1$ ,  $n = 38$  for hH1/ $\beta_{122}$ , and  $n = 50$  for hH1/ $\beta_{211}$ ). (C) Time course of recovery from the inactivation of hH1 channels ( $n = 7$  for hH1,  $n = 6$  for hH1/ $\beta_1$ ,  $n = 5$  for hH1/ $\beta_{122}$ , and  $n = 6$  for hH1/ $\beta_{211}$ ). (D) Effect of  $\beta_{122}$  on the inactivation time course of rat brain IIA  $\text{Na}^+$  currents (test pulse:  $-10$  mV). Calibration bars = 5 ms,  $0.25 \mu\text{A}$  for IIA,  $0.52 \mu\text{A}$  for IIA/ $\beta_1$ ,  $0.27 \mu\text{A}$  for IIA/ $\beta_{122}$ , and  $0.21 \mu\text{A}$  for IIA/ $\beta_{211}$ . (E) Effect of  $\beta_{122}$  on the IIA peak current amplitude (test pulse to  $-10$  mV;  $*P < 0.001$ ;  $n = 19$  for IIA,  $n = 13$  for IIA/ $\beta_1$ ,  $n = 19$  for IIA/ $\beta_{122}$ , and  $n = 17$  for IIA/ $\beta_{211}$ ). (F) Time course of recovery from inactivation of IIA channels. For voltage protocol, see legend to Fig. 1 ( $n = 13$  for IIA,  $n = 12$  for IIA/ $\beta_1$  and  $n = 12$  for IIA/ $\beta_{122}$ , and  $n = 12$  for IIA/ $\beta_{211}$ ). Bars indicate SEM.

TABLE I  
Effect of the Different  $\beta$  Subunit Constructs on Current Density  
and Recovery from Inactivation of hH1 Channels

Channels	$I_{\max}^a$	$\tau_{\text{rec}}^b$
		ms
hH1	1	$5.87 \pm 0.18$
hH1/ $\beta_1$	$3.47 \pm 0.32^c$	$3.20 \pm 0.13^c$
hH1/ $\beta_2$	$0.86 \pm 0.50$	$5.79 \pm 0.47$
hH1/ $\beta_{122}$	$1.03 \pm 0.15$	$5.24 \pm 0.27$
hH1/ $\beta_{211}$	$2.26 \pm 0.18^c$	$3.74 \pm 0.23^c$
hH1/ $\beta_{122a}$	$1.22 \pm 0.30$	$5.30 \pm 0.17$
hH1/ $\beta_{211a}$	$2.61 \pm 0.48^c$	$3.33 \pm 0.04^c$
hH1/ $\beta_{121}$	$1.16 \pm 0.11$	$5.01 \pm 0.37^c$
hH1/ $\beta_{212}$	$0.88 \pm 0.07$	$5.31 \pm 0.23$
hH1/ $\beta_{221}$	$1.19 \pm 0.11$	$4.79 \pm 0.45^c$
hH1/ $\beta_{11\Delta}$	$1.33 \pm 0.15^c$	$3.95 \pm 0.29^c$
hH1/ $\beta_{12\Delta}$	$0.81 \pm 0.21$	$5.58 \pm 0.30$
hH1/ $\beta_{21\Delta}$	$0.78 \pm 0.06$	$5.70 \pm 1.10$

<sup>a</sup>Peak current amplitudes relative to hH1.

<sup>b</sup>Recovery time constants  $\tau_{\text{rec}}$  determined with monoexponential fits.

<sup>c</sup>Significantly different compared to hH1 channels ( $P < 0.05$ ).

### Electrophysiology

Whole-cell  $\text{Na}^+$  currents were recorded with the two-microelectrode voltage clamp technique using a commercial amplifier (OC725C; Warner Instruments Corp.). Glass microelectrodes were filled with 3 M KCl solution. The microelectrode resistance was between 0.2 and 0.5 M $\Omega$ . The bath solution contained (in mM): 20 NaCl, 97.5 KCl, 1.8 CaCl<sub>2</sub>, 10 HEPES/KOH, pH 7.2. The currents were elicited by test potentials from  $-80$  to  $40$  mV in 5-mV increments from a holding potential of  $-120$  mV. The pulsing frequency was 0.2 Hz. Recovery from inactivation was determined with a standard protocol (Fig. 1 C, inset) at a frequency of 0.2 Hz. The amplitude of  $I_{\text{Na}}$ , measured 3 d after injection at the test potential of  $-25$  mV (hH1) and  $-10$  mV (IIA) was between 0.5 to 5.0  $\mu\text{A}$ . The recovery from inactivation was determined from  $\text{Na}^+$  currents with an amplitude between 1.5 to 3  $\mu\text{A}$ . Recording and analysis of the data were performed on a PC with the ISO2 software (MFK). The sampling rate was 20 kHz.

### Statistics

Student's *t* test was applied to test for statistical significance using the Microcal Origin 5.0 software (Microcal Software, Inc.). Statistical significance was assumed for  $P < 0.05$ .

## RESULTS

### The $\beta_1$ Subunit Modulates both hH1 and IIA Channels

We first analyzed the effects of the  $\beta_1$  and  $\beta_2$  subunit on the current density, the recovery from inactivation, and the time course of inactivation in both hH1 and IIA currents. We found that the  $\beta_2$  subunit neither modulated hH1 nor IIA channels (Fig. 1). In contrast, the  $\beta_1$  subunit produced significantly larger whole-cell currents (Fig. 1, B and E) and accelerated recovery from inactivation of both hH1 and IIA channels (Fig. 1, C and F). In addition to this, we observed rapidly inacti-

vating  $\text{Na}^+$  currents in IIA/ $\beta_1$  channels that were not seen when expressing IIA channels alone (Fig. 1 D). A statistically significant effect of the  $\beta_1$  subunit on hH1 inactivation was not observed (Fig. 1 A).

The similarity of the  $\beta_1$  subunit effects on current density and recovery from inactivation of the cardiac and brain  $\text{Na}^+$  channels suggests a similar mechanism for the  $\alpha/\beta_1$  subunit interaction. We tested this hypothesis by coexpressing various  $\beta_1/\beta_2$  subunit chimeras (Fig. 2) with hH1 and IIA channels in the oocyte system. Although both  $\beta$  subunits share little contiguous primary sequence similarity ( $\sim 14\%$  identity throughout the sequences), their conformation and topology are presumably very similar (Isom et al., 1992; Isom et al., 1995). Both subunits are predicted to be membrane anchored, exposing the larger  $\text{NH}_2$ -terminal domain to the extracellular side and the smaller  $\text{COOH}$ -terminal region into the cytosol (Fig. 2).

### hH1 and IIA Channels Are Modulated by Different $\beta_1$ Subunit Regions

Coexpression of chimera  $\beta_{122}$  that consisted of the  $\beta_1$  extracellular domain (ED), the  $\beta_2$  membrane anchor (MA) and the  $\beta_2$  intracellular domain (ID; see Figs. 2 and 3 A) did neither enhance the current density nor accelerate the recovery from inactivation of hH1 channels (Fig. 3, B and C). In contrast,  $\beta_1$ -like effects on hH1 currents were observed when coexpressing the opposite chimera  $\beta_{211}$ , indicating that the MA plus the ID of the  $\beta_1$  subunit are required to modulate hH1 channels (Fig. 3, B and C, Table I). In control experiments, we tested the effect of both chimeras on IIA channels and observed that only  $\beta_{122}$ , but not  $\beta_{211}$ , modulated the inactivation time course, current density, and recovery from inactivation (Fig. 3, D–F). This indicates that the  $\beta_1$  ED is necessary and sufficient to modulate IIA channels, similarly as reported previously (McCormick et al., 1999). Coexpression of  $\beta_{211}$ , however, that was sufficient to modulate hH1, had no effect on IIA channels (Fig. 3, B and C). The same results were obtained when using a structurally similar pair of  $\beta$  subunit chimeras ( $\beta_{122a}$  and  $\beta_{211a}$  in Fig. 2; Table I). In conclusion, the cardiac  $\text{Na}^+$  channel isoform hH1 is modulated by the  $\beta_1$  MA plus the ID, whereas the  $\beta_1$  ED was sufficient to modulate the neuronal isoform IIA.

### The $\beta_1$ Intracellular Domain Requires its Own Membrane Anchor for Full Effect on hH1

To test whether or not the  $\beta_1$  ID is sufficient to modulate hH1 currents, two chimeras were constructed that contained the  $\beta_1$  ID, the  $\beta_2$  MA, and either the  $\beta_1$  or the  $\beta_2$  ED ( $\beta_{121}$  and  $\beta_{221}$ ; Fig. 4 A). As result, none of the chimeras increased the hH1 current density (Fig. 4 B). We observed a moderate but significant acceleration of recovery from inactivation that was, however, significantly less

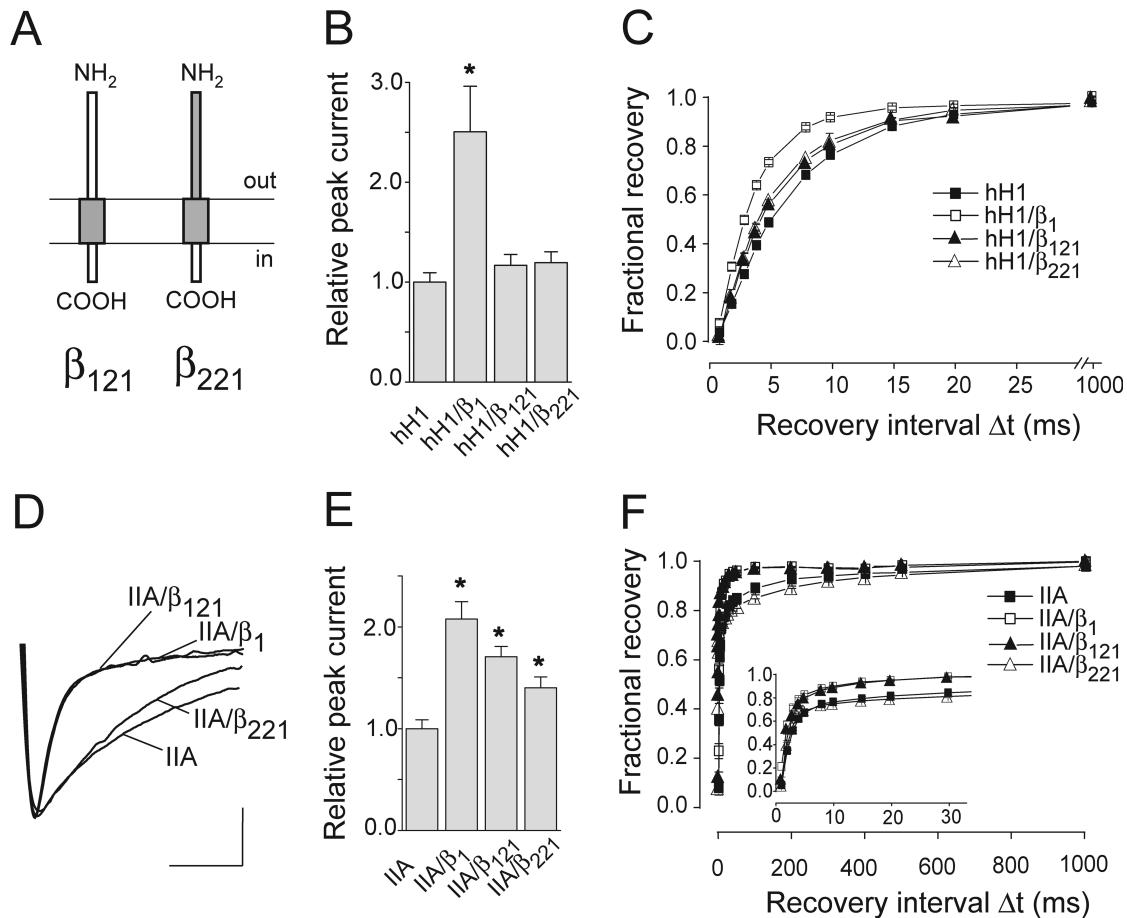


FIGURE 4. Coexpression of chimeras  $\beta_{121}$  and  $\beta_{221}$  with hH1 and IIA channels. (A) Schematic representation of the domain structures of both chimeras. (B) Relative current amplitudes (test pulse to  $-25$  mV; \* $P < 0.001$ ;  $n = 29$  for hH1,  $n = 17$  for hH1/ $\beta_1$ ,  $n = 28$  for hH1/ $\beta_{121}$ , and  $n = 21$  for hH1/ $\beta_{221}$ ). (C) Time course of recovery from inactivation of hH1 channels ( $n = 21$  for hH1,  $n = 17$  for hH1/ $\beta_1$ ,  $n = 12$  for hH1/ $\beta_{121}$ , and  $n = 19$  for hH1/ $\beta_{221}$ ). (D) Effect of  $\beta_{121}$  on the time course of inactivation of rat brain IIA  $\text{Na}^+$  currents (test pulse to  $-10$  mV). Calibration bars = 5 ms,  $0.93 \mu\text{A}$  for IIA,  $0.90 \mu\text{A}$  for IIA/ $\beta_1$ ,  $0.62 \mu\text{A}$  for IIA/ $\beta_{121}$ , and  $0.90 \mu\text{A}$  for IIA/ $\beta_{221}$ . (E) Effect of  $\beta_{121}$  and  $\beta_{221}$  on the IIA peak current amplitude (test pulse to  $-10$  mV; \* $P < 0.001$ ;  $n = 15$  for IIA,  $n = 9$  for IIA/ $\beta_1$ ,  $n = 12$  for IIA/ $\beta_{121}$ , and  $n = 19$  for IIA/ $\beta_{221}$ ). (F) Time course of recovery from inactivation of IIA channels ( $n = 13$  for IIA,  $n = 9$  for IIA/ $\beta_1$  and  $n = 5$  for IIA/ $\beta_{121}$ , and  $n = 13$  for IIA/ $\beta_{221}$ ). Bars indicate SEM.

pronounced compared with the effect of the wild-type  $\beta_1$  subunit (Fig. 4 C, Table I). In parallel experiments with IIA channels,  $\beta_{121}$  induced the full  $\beta_1$  effect on IIA inactivation, current density, and recovery from inactivation (Fig. 4, D–F). These results indicate that the  $\beta_1$  ED in the  $\beta_{121}$  chimera was functionally active to modulate IIA channels. As expected, chimera  $\beta_{221}$  had no effect on the inactivation time course (Fig. 4 D) and the recovery from inactivation (Fig. 4 F) of IIA currents. Interestingly, we found a small but significant increase of the IIA current density (Fig. 4 E), suggesting that also the  $\beta_1$  ID modulates the current density of IIA channels.

Considering the results with hH1, the exchange of the  $\beta_1$  MA by the corresponding  $\beta_2$  MA disturbed the  $\beta_1$ -like effects ( $\beta_1$  versus  $\beta_{121}$ , Fig. 4;  $\beta_{211}$  versus  $\beta_{221}$ , Figs. 3 and 4, Table I). Hence, the  $\beta_1$  MA plays a crucial role in the interaction of the  $\beta_1$  subunit with hH1. However, when fused to the ED and the ID of the  $\beta_2$

subunit, the  $\beta_1$  MA alone did neither enhance current density nor accelerate recovery from inactivation of hH1 currents ( $\beta_{212}$ , Fig. 5, Table I). Similar results were obtained with a deletion mutant consisting of the  $\beta_2$  ED plus the  $\beta_1$  MA ( $\beta_{21\Delta}$ , Fig. 5, Table I), confirming that the  $\beta_1$  MA is not sufficient to modulate hH1 currents. In addition to this membrane-spanning region, the  $\beta_1$  ID is required for an efficient modulation of hH1 channels ( $\beta_{21\Delta}$  vs.  $\beta_{211}$ , Figs. 3 and 5, Table I).

*The  $\beta_1$  Extracellular Domain Plus the  $\beta_1$  Membrane Anchor has Partially  $\beta_1$ -like Effects on hH1*

Because the  $\beta_1$  ID efficiently modulates hH1 channels only when linked to the  $\beta_1$  MA, we tested whether also the  $\beta_1$  ED requires the fusion to the  $\beta_1$  MA in order to functionally interact with hH1. To address this question we fused the  $\beta_1$  ED either to the  $\beta_1$  or to the  $\beta_2$  MA (resulting in  $\beta_{11\Delta}$  or  $\beta_{12\Delta}$ , respectively), and expressed

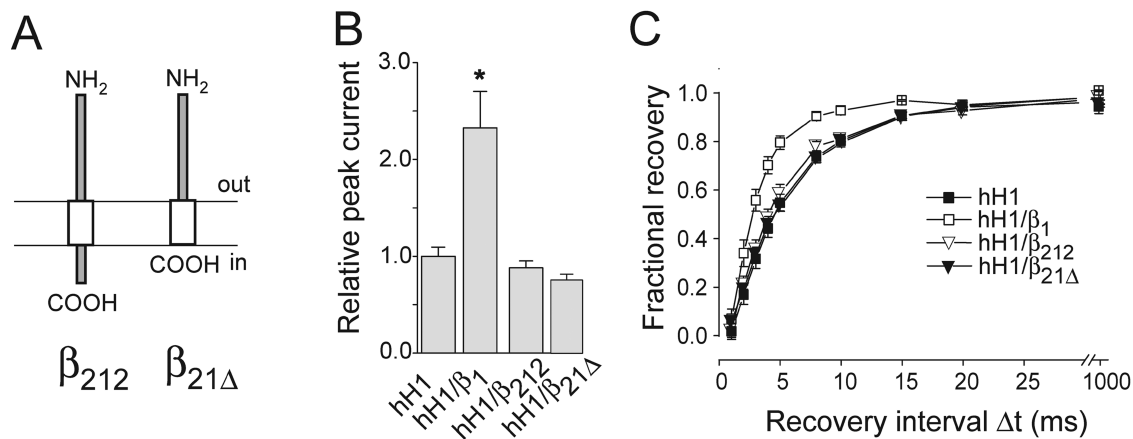


FIGURE 5. Coexpression of chimera  $\beta_{212}$  and  $\beta_{21\Delta}$  with hH1 channels. (A) Schematic representation of the domain structure of  $\beta_{212}$  and  $\beta_{21\Delta}$ . (B) Relative current amplitudes (test pulse to -25 mV; \* $P < 0.001$ ;  $n = 17$  for hH1,  $n = 10$  for hH1/ $\beta_1$ ,  $n = 21$  for hH1/ $\beta_{212}$ , and  $n = 11$  for  $\beta_{21\Delta}$ ). (C) Time course of recovery from inactivation of hH1 channels ( $n = 10$  for hH1,  $n = 4$  for hH1/ $\beta_1$ ,  $n = 11$  for hH1/ $\beta_{212}$ , and  $n = 7$  for  $\beta_{21\Delta}$ ). Bars indicate SEM.

these deletion variants lacking the  $\beta_1$  ID with hH1 or IIA channels (Fig. 6 A).

As a result,  $\beta_{11\Delta}$  accelerated the recovery from inactivation of hH1 currents (Fig. 6, B and C, Table I). In contrast to this, coexpression of  $\beta_{12\Delta}$  did not produce  $\beta_1$ -like effects on hH1. This result shows that the  $\beta_1$  MA is required in  $\beta_{11\Delta}$  to modulate hH1 channels. In  $\beta_{11\Delta}$ , a few amino acids are probably exposed to the intracellular side, thus belonging to the ID. These residues should, however, not be responsible for the modulation of hH1, because the same amino acids are present in  $\beta_{21\Delta}$  which had no effect on hH1 (Fig. 5).

In case of IIA channels, both  $\beta_{11\Delta}$  and  $\beta_{12\Delta}$  accelerated the inactivation time course and the recovery process from inactivation (Fig. 6, D–F), again confirming that the  $\beta_1$  ED suffices to modulate IIA channels.

Although the hH1 and IIA current amplitudes increased significantly when coexpressing  $\beta_{11\Delta}$ , respective values were clearly smaller compared with the data obtained with hH1/ $\beta_1$  or IIA/ $\beta_1$  channels (Fig. 6, B and E). Thus, the absence of the  $\beta_1$  ID caused a partial loss of function, suggesting an  $\alpha/\beta_1$  subunit interaction on the cytoplasmic side.

## DISCUSSION

In the present study we took advantage of the nonmodulating  $\beta_2$  subunit to explore molecular regions of the  $\beta_1$  subunit that functionally interact with hH1 to enhance current density and to accelerate recovery from inactivation. Coexpression of  $\beta_1/\beta_2$  subunit chimeras and deletion variants revealed that the functional  $\alpha/\beta_1$  interaction is not mediated by a conserved molecular mechanism in IIA and hH1 channels. In contrast to the results obtained with the Na<sup>+</sup> channel isoforms of brain (McCormick et al., 1998, 1999; this study) and skeletal mus-

cle (Chen and Cannon, 1995), the extracellular domain of the  $\beta_1$  subunit was neither sufficient nor required to modulate the cardiac-specific Na<sup>+</sup> channel isoform. Instead, the  $\beta_1$  membrane anchor was identified as a structural requirement for  $\beta_1$ -like modulation of hH1. All chimeras lacking this region failed to increase current density and to accelerate recovery from inactivation.

However, the  $\beta_1$  membrane anchor alone did not modulate hH1 currents (see  $\beta_{212}$  in Fig. 5). To accelerate the recovery process, additional molecular regions of the  $\beta_1$  subunit were necessary: either the ID in  $\beta_{211}$  or the ED in  $\beta_{11\Delta}$ . This surprising result suggests two alternative mechanisms for the acceleration of the recovery from inactivation: one mediated by extracellular and the other by intracellular hH1/ $\beta_1$  interaction sites. Both mechanisms obviously require the primary interaction of the  $\beta_1$  membrane-spanning region with a putative intramembrane site in hH1. This interaction could then facilitate an exposure of the ID and the ED of the  $\beta_1$  subunit to respective interaction sites of hH1, finally resulting in a specific hH1/ $\beta_1$  interaction and in the observed current modulation.

In addition to the effect on the recovery of hH1 channels, a strong increase in the current density was only observed with the wild-type  $\beta_1$  subunit and with chimera  $\beta_{211}$  (see Fig. 3). Deletion of the  $\beta_1$  intracellular domain ( $\beta_{11\Delta}$  and  $\beta_{21\Delta}$ ) significantly reduced the peak current amplitude, suggesting an important role of the  $\beta_1$  intracellular domain for an efficient hH1/ $\beta_1$  subunit interaction. We speculate that the absence of this domain reduces the binding affinity between  $\beta_1$  and hH1, finally resulting in a decreased cell surface expression of functional channels. Supporting this view, Meadows et al. (2001) recently showed by coimmunoprecipitation experiments that the deletion of 34 amino acids at the COOH terminus of the  $\beta_1$  subunit

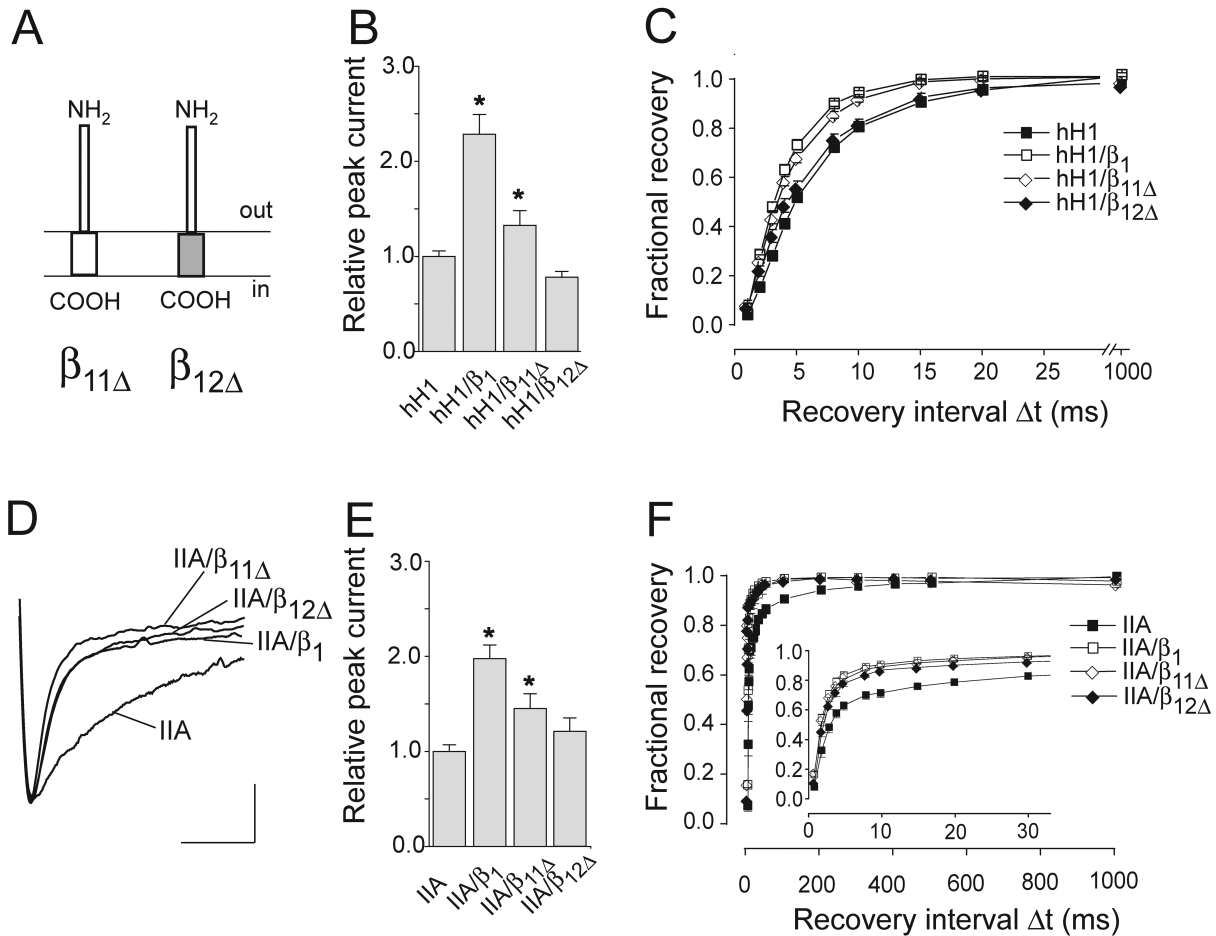


**FIGURE 6.** Coexpression of  $\beta_{11\Delta}$  and  $\beta_{12\Delta}$  with hH1 and IIA channels. (A) Schematic representation of the domain structures of both deletion variants. (B) Relative current amplitudes (test pulse to  $-25$  mV; \* $P < 0.001$ ;  $n = 38$  for hH1,  $n = 38$  for hH1/ $\beta_1$ ,  $n = 30$  for hH1/ $\beta_{11\Delta}$ , and  $n = 23$  for hH1/ $\beta_{12\Delta}$ ). (C) Time course of recovery from inactivation of hH1 channels ( $n = 23$  for hH1,  $n = 21$  for hH1/ $\beta_1$ ,  $n = 19$  for hH1/ $\beta_{11\Delta}$ , and  $n = 20$  for hH1/ $\beta_{12\Delta}$ ). (D) Effect of  $\beta_{11\Delta}$  and  $\beta_{12\Delta}$  on the inactivation time course of rat brain IIA Na<sup>+</sup> currents (test pulse to  $-10$  mV). Calibration bars = 5 ms, 0.92  $\mu$ A for IIA, 0.76  $\mu$ A for IIA/ $\beta_1$ , 0.80  $\mu$ A for IIA/ $\beta_{11\Delta}$ , and 0.28  $\mu$ A for IIA/ $\beta_{12\Delta}$ . (E) Effect of  $\beta_{11\Delta}$  and  $\beta_{12\Delta}$  on the IIA peak current amplitude (test pulse to  $-10$  mV; \* $P < 0.001$ ;  $n = 16$  for IIA,  $n = 14$  for IIA/ $\beta_1$ ,  $n = 21$  for IIA/ $\beta_{11\Delta}$ , and  $n = 9$  for IIA/ $\beta_{12\Delta}$ ). (F) Time course of recovery from inactivation of IIA channels ( $n = 13$  for IIA,  $n = 13$  for IIA/ $\beta_1$ ,  $n = 16$  for IIA/ $\beta_{11\Delta}$ , and  $n = 10$  for IIA/ $\beta_{12\Delta}$ ). Bars indicate SEM.

drastically reduced the  $\beta_1$  binding affinity to IIA channels in a mammalian cell line.

The intracellular  $\beta_1$  domain may exert its effect on hH1 channels not only by a direct subunit interaction, but also through the interaction with other proteins. Recent studies provided evidence for cytoskeletal interactions of the  $\beta_1$  subunit through ankyrin (Chauhan et al., 2000; Malhotra et al., 2000) and for the binding of the  $\beta_1$ , but not the  $\beta_2$  subunit, to receptor tyrosine phosphatase  $\beta$  (Ratcliffe et al., 2000). Thus, the hH1/ $\beta_1$  interaction at the intracellular side might be regulated by cytoskeletal proteins or by a specific phosphorylation site in the  $\beta_1$  intracellular domain.

Recently, an alternative spliced variant of the  $\beta_1$  subunit has been reported ( $\beta_{1A}$ ; Kazen-Gillespie et al., 2000), which is expressed in the heart. Similar to the  $\beta_2$  subunit, this splice variant possesses a membrane-spanning and intracellular domain that shows no obvious

sequence similarities with the respective regions of the  $\beta_1$  subunit (protein sequence identity of 10.5% and 8.6% of the  $\beta_{1A}$  ID vs. the corresponding residues in  $\beta_1$  and  $\beta_2$ , respectively). Therefore, it is likely that  $\beta_{1A}$  has either no or at least altered modulating effects on hH1. Respective coexpression studies with hH1/ $\beta_{1A}$  channels including  $\beta_1$ / $\beta_{1A}$  chimeras could be a clue for the understanding of the physiological relevance of the alternative splicing of the  $\beta_1$  subunit in the heart.

In conclusion, our data contribute to a better understanding of the hH1/ $\beta_1$  interaction. We provide evidence that different molecular mechanisms underlie the  $\beta_1$  modulatory effects in hH1/ $\beta_1$  and IIA/ $\beta_1$  channels. Future studies using site-directed mutagenesis and protein binding assays may reveal the corresponding key amino acids both in hH1 and in the  $\beta_1$  subunit that determine the nature of the subunit interaction of the cardiac Na<sup>+</sup> channel.



The authors are grateful to K. Schoknecht for her contribution to the electrophysiological recordings, and to S. Bernhardt, A. Kolchmeier, and B. Tietsch for their technical assistance.

This work was supported by grant Be1250/9-2 from the Deutsche Forschungsgemeinschaft to K. Benndorf and T. Zimmer, and by BMBF grant 01ZZ015/IZKF Jena to T. Zimmer.

Submitted: 23 August 2002

Revised: 17 October 2002

Accepted: 21 October 2002

#### REFERENCES

- Auld, V.J., A.L. Goldin, D.S. Krafte, J. Marshall, J.M. Dunn, W.A. Catterall, H.A. Lester, N. Davidson, and R.J. Dunn. 1988. A rat brain Na<sup>+</sup> channel  $\alpha$  subunit with novel gating properties. *Neuron*. 1:449–461.
- Catterall, W.A. 1992. Cellular and molecular biology of voltage-gated sodium channels. *Physiol. Rev.* 72:S15–S48.
- Chauhan, V.S., S. Tuvia, M. Buhusi, V. Bennett, and A.O. Grant. 2000. Abnormal cardiac Na<sup>+</sup> channel properties and QT heart rate adaptation in neonatal ankyrin<sub>B</sub> knockout mice. *Circ. Res.* 86:441–447.
- Chen, C., and S.C. Cannon. 1995. Modulation of Na<sup>+</sup> channel inactivation by the  $\beta_1$  subunit: a deletion analysis. *Pflugers Arch.* 431:186–195.
- Gellens, M.E., A.L. George, L. Chen, M. Chahine, R. Horn, R.L. Barchi, and R.G. Kallen. 1992. Primary structure and functional expression of the human cardiac tetrodotoxin-insensitive voltage-dependent sodium channel. *Proc. Natl. Acad. Sci. USA.* 89:554–558.
- Goldin, A.L. 2001. Resurgence of sodium channel research. *Annu. Rev. Physiol.* 63:871–894.
- Higuchi, R. 1989. Using PCR to engineer DNA. In *PCR Technology: Principles and Applications for DNA Amplification*. H.A. Erlich, editor. Stockton Press, NY. 61–70.
- Isom, L.L. 2001. Sodium channel  $\beta$  subunits: anything but auxiliary. *Neuroscientist.* 7:42–51.
- Isom, L.L., K.S. De Jongh, D.E. Patton, B.F.X. Reber, J. Offord, H. Charbonneau, K. Walsh, A.L. Goldin, and W.A. Catterall. 1992. Primary structure and functional expression of the  $\beta_1$  subunit of the rat brain sodium channel. *Science.* 256:839–842.
- Isom, L.L., D.S. Ragsdale, K.S. De Jongh, R.E. Westenbroek, B.F.X. Reber, T. Scheuer, and W.A. Catterall. 1995. Structure and function of the  $\beta_2$  subunit of brain sodium channels, a transmembrane glycoprotein with a CAM motif. *Cell.* 83:433–442.
- Kazen-Gillespie, K.A., D.S. Ragsdale, M.R. D'Andrea, L.N. Mattei, K.E. Rogers, and L.L. Isom. 2000. Cloning, localization, and functional expression of sodium channel  $\beta_1A$  subunits. *J. Biol. Chem.* 275:1079–1088.
- Liman, E.R., J. Tytgat, and P. Hess. 1992. Subunit stoichiometry of a mammalian K<sup>+</sup> channel determined by construction of multimeric cDNAs. *Neuron.* 9:861–871.
- Makita, N., P.B. Bennett, and A.L. George. 1994. Voltage-gated Na<sup>+</sup> channel  $\beta_1$  subunit mRNA expressed in adult human skeletal muscle, heart, and brain is encoded by a single gene. *J. Biol. Chem.* 269:7571–7578.
- Makita, N., P.B. Bennett, and A.L. George. 1996. Molecular determinants of  $\beta_1$  subunit-induced gating modulation in voltage-dependent Na<sup>+</sup> channels. *J. Neurosci.* 16:7117–7127.
- Malhotra, J.D., K. Kazen-Gillespie, M. Hortsch, and L.L. Isom. 2000. Sodium channel  $\beta$  subunits mediate homophilic cell adhesion and recruit ankyrin to points of cell-cell contact. *J. Biol. Chem.* 275:11383–11388.
- McCormick, K.A., L.L. Isom, D. Ragsdale, D. Smith, T. Scheuer, and W.A. Catterall. 1998. Molecular determinants of Na<sup>+</sup> channel function in the extracellular domain of the  $\beta_1$  subunit. *J. Biol. Chem.* 273:3954–3962.
- McCormick, K.A., J. Srinivasan, K. White, T. Scheuer, and W.A. Catterall. 1999. The extracellular domain of the  $\beta_1$  subunit is both necessary and sufficient for  $\beta_1$ -like modulation of sodium channel gating. *J. Biol. Chem.* 274:32638–32646.
- Meadows, L., J.D. Malhotra, A. Stetzer, L.L. Isom, and D.S. Ragsdale. 2001. The intracellular segment of the sodium channel  $\beta_1$  subunit is required for its efficient association with the channel  $\alpha$  subunit. *J. Neurochem.* 76:1871–1878.
- Morgan, K., E.B. Stevens, B. Shah, P.J. Cox, A.K. Dixon, K. Lee, R.D. Pinnock, J. Hughes, P.J. Richardson, K. Mizuguchi, and A.P. Jackson. 2000.  $\beta_3$ : An additional auxiliary subunit of the voltage-sensitive sodium channel that modulates channel gating with distinct kinetics. *Proc. Natl. Acad. Sci. USA.* 97:2308–2313.
- Nuss, H.B., N. Chiamvimonvat, M.T. Perez-Garcia, G.F. Tomaselli, and E. Marban. 1995. Functional association of the  $\beta_1$  subunit with human cardiac (hH1) and rat skeletal muscle ( $\mu_1$ ) sodium channel  $\alpha$  subunits expressed in *Xenopus* oocytes. *J. Gen. Physiol.* 106:1171–1191.
- Patton, D.E., L.L. Isom, W.A. Catterall, and A.L. Goldin. 1994. The adult rat brain  $\beta_1$  subunit modifies activation and inactivation gating of multiple sodium channel  $\alpha$  subunits. *J. Biol. Chem.* 269:17649–17655.
- Qu, Y., L.L. Isom, R.E. Westenbroek, J.C. Rogers, T.N. Tanada, K.A. McCormick, T. Scheuer, and W.A. Catterall. 1995. Modulation of cardiac Na<sup>+</sup> channel expression in *Xenopus* oocytes by  $\beta_1$  subunits. *J. Biol. Chem.* 270:25696–25701.
- Qu, Y., J.C. Rogers, S.-F. Chen, K.A. McCormick, T. Scheuer, and W.A. Catterall. 1999. Functional roles of the extracellular segments of the sodium channel  $\alpha$  subunit in voltage-dependent gating and modulation by  $\beta_1$  subunits. *J. Biol. Chem.* 274:32647–32654.
- Ratcliffe, C.F., Y. Qu, K.A. McCormick, V.C. Tibbs, J.E. Dixon, T. Scheuer, and W.A. Catterall. 2000. A sodium channel signaling complex: modulation by associated receptor protein tyrosine phosphatase beta. *Nat. Neurosci.* 3:437–444.
- Sambrook, J., E.F. Fritsch, and T. Maniatis. 1989. *Molecular Cloning: A Laboratory Manual*. Cold Spring Harbor Laboratory Press, Cold Spring Harbor, NY.
- Smith, R.D., and A.L. Goldin. 1998. Functional analysis of the rat I sodium channel in *Xenopus* oocytes. *J. Neurosci.* 18:811–820.
- Srinivasan, J., M. Schachner, and W.A. Catterall. 1998. Interaction of voltage-gated sodium channels with the extracellular matrix molecules tenascin-C and tenascin-R. *Proc. Natl. Acad. Sci. USA.* 95:15753–15757.
- Vijayaragavan, K., M.E. O'Leary, and M. Chahine. 2001. Gating properties of Na<sub>v</sub>1.7 and Na<sub>v</sub>1.8 peripheral nerve sodium channels. *J. Neurosci.* 21:7909–7918.
- Wallner, M., L. Weigl, P. Meera, and I. Lotan. 1993. Modulation of the skeletal muscle sodium channel  $\alpha$ -subunit by the  $\beta_1$ -subunit. *FEBS Lett.* 336:535–539.
- Xiao, Z.-C., D.S. Ragsdale, J.D. Malhotra, L.N. Mattei, P.E. Braun, M. Schachner, and L.L. Isom. 1999. Tenascin-R is a functional modulator of sodium channel  $\beta$  subunits. *J. Biol. Chem.* 274:26511–26517.
- Yang, J.S., P.B. Bennett, N. Makita, A.L. George, and R.L. Barchi. 1993. Expression of the sodium channel  $\beta_1$  subunit in rat skeletal muscle is selectively associated with the tetrodotoxin-sensitive  $\alpha$  subunit isoform. *Neuron.* 11:915–922.
- Zerangue, N., B. Schwappach, Y.N. Jan, and L.Y. Jan. 1999. A new ER trafficking signal regulates the subunit stoichiometry of plasma membrane K<sub>ATP</sub> channels. *Neuron.* 22:537–548.
- Zimmer, T., C. Biskup, C. Bollensdorff, and K. Benndorf. 2002. The  $\beta_1$  subunit but not the  $\beta_2$  subunit colocalizes with the human heart Na<sup>+</sup> channel (hH1) already within the endoplasmic reticulum. *J. Membr. Biol.* 186:13–21.